The value of $(\epsilon/k)_i$ determines the critical temperature in each layer, whereas U_i determines the position of the step on the pressure axis. Sinanoglu and Pitzer[23] have determined using third-order perturbation theory that the pairwise interactions of molecules adsorbed on a surface in the submonolayer region are less than in the gas phase. These results are in good agreement with their theory as their theory predicts a 20–40% reduction in the gas-phase Lennard-Jones potential minimum. The critical temperatures predicted by the present treatment are about 65°K for the first layer and 68°K for the second layer. This brings up the very interesting situation where at points intermediate between these two temperatures the first layer is supercritical and the second layer is subcritical. Unfortunately not enough data have been taken with the Ar–BN system to verify whether this is indeed possible. If so, then a smooth transition is seen to take place between the adsorbed state and the liquid state.

The value of U_1 used is very close to that estimated for the Ar–BN system by Pierotti[3] using the Frenkel–Halsey–Hill equation. No independent values are available for U_2 or U_3.

The significant structure theory is often criticized for the intuitive nature of its development and the number of adjustable parameters in the partition functions. Here only U_i is adjusted to fit the data, and, as pointed out by McAlpin and Pierotti,[7] the more or less arbitrary parameter n_h used in the liquid theory is in an adsorption theory related to the experimentally measurable surface coverage. The extraordinarily realistic fit provided in the present case can only lend more credit to this theory.

References and Notes

(1) This work was in part done in partial fulfillment of the requirements for a Ph.D. Degree at the Department of Chemistry, Georgia Institute of Technology, 1972.
(2) (a) A. Thomy and X. Duval, *J. Chim. Phys.*, **67**, 1101 (1970); (b) S. Ross and W. Winkler, *J. Colloid Sci.*, **10**, 330 (1955).
(3) R. A. Pierotti, *J. Phys. Chem.*, **66**, 1810 (1962).
(4) C. F. Prenzlow and G. D. Halsey, Jr., *J. Phys. Chem.*, **61**, 1158 (1957).
(5) J. H. Singleton and G. D. Halsey, Jr., *J. Phys. Chem.*, **58**, 1011 (1954).
(6) W. A. Steele, *J. Phys. Chem.*, **69**, 3446 (1965).
(7) J. J. McAlpin and R. A. Pierotti, *J. Chem. Phys.*, **41**, 68 (1964).
(8) J. J. McAlpin and R. A. Pierotti, *J. Chem. Phys.*, **42**, 1842 (1965).
(9) J. R. Sams, G. Constabaris, and G. D. Halsey, Jr., *J. Chem. Phys.*, **36**, 1334 (1962).
(10) R. N. Ramsey, H. E. Thomas, and R. A. Pierotti, *J. Phys. Chem.*, **76**, 3171 (1972).
(11) W. A. Steele, *Surface Sci.*, **39**, 149 (1973).
(12) E. L. Pace, *J. Chem. Phys.*, **27**, 1341 (1957).
(13) R. A. Beebe and D. M. Young, *J. Phys. Chem.*, **58**, 93 (1954).
(14) R. A. Pierotti and H. E. Thomas, "Surface and Colloid Science," Vol. IV, Wiley-Interscience, New York, N.Y., 1971, pp 93–259.
(15) L. A. Bruce and M. H. Sheridan, *J. Chem. Soc., Faraday Trans. 1*, **69**, 176 (1973).
(16) H. Eyring, T. Ree, and N. Hirai, *Proc. Nat. Acad. Sci. U. S.*, **44**, 683 (1958).
(17) H. Eyring and M. S. Jhon, "Significant Liquid Structures," Wiley, New York, N.Y., 1969, Chapter 3.
(18) D. Henderson, *J. Chem. Phys.*, **39**, 1857 (1963).
(19) J. E. Lennard-Jones and A. F. Devonshire, *Proc. Roy. Soc., Ser. A*, **163**, 53 (1937).
(20) A. F. Devonshire, *Proc. Roy. Soc., Ser. A*, **163**, 132 (1937).
(21) S. Ross and W. W. Pultz, *J. Colloid Sci.*, **13**, 397 (1958).
(22) J. O. Hirschfelder, C. F. Curtiss, and R. B. Bird, "Molecular Theory of Gases and Liquids," Wiley, New York, N.Y., 1954, p 1110.
(23) O. Sinanoglu and K. S. Pitzer, *J. Chem. Phys.*, **32**, 1729 (1960).

Electronic Structures of Cephalosporins and Penicillins. III. EH and CNDO/2D Electron Density Maps of 7-Amino-3-cephem

Donald B. Boyd

Lilly Research Laboratories, Eli Lilly and Company, Indianapolis, Indiana 46206

(Received July 9, 1974)

Publication costs assisted by Eli Lilly and Company

Contour maps of electron density computed from EH (extended Hückel) and CNDO/2D (complete-neglect-of-differential-overlap, deorthogonalized) wave functions are reported for the molecular nucleus of cephalosporin antibiotics. Density is computed in planes through the sulfide, ethylenic, and β-lactam functionalities. Comparison of the two MO methods reveals qualitative similarities for most of the charge distributions, but interestingly, CNDO/2D gives greater directionality to the lone pairs on S, N, and O. The charge distributions are discussed in relation to the mechanism of biological activity of β-lactam antibiotics.

Introduction

Recent utilizations of molecular orbital methods in studying structure–activity relationships among β-lactam antibiotics have extended the understanding of the electronic structures of cephalosporins and penicillins. In the first paper of this series, extended Hückel (EH) wave functions were used to assign the uv and circular dichroism bands of cephalosporins, penicillins, and related structures.[1] Despite the simplicity of the theory, reasonable correlations of predicted and experimental absorptions were obtained. In the second paper of the series, the EH charge distributions in the β-lactam ring were correlated with biological activity of antibiotics with different molecular nuclei.[2] A deficiency of electron density on the carbonyl carbon and a lability of the β-lactam C–N bond were found to be among the attributes of good antibiotics. In other words,

the β-lactam ring must have a certain degree of susceptibility to nucleophilic attack for high biological activity. Our findings are consistent with the proposed mode of action of the β-lactam antibiotics; namely, they acylate and thereby inactivate a transpeptidase involved in bacterial cell wall synthesis.[3] The main conclusions regarding the EH derived charge distributions are corroborated in studies using another popular semiempirical MO method, CNDO/2 (complete-neglect-of-differential-overlap).[4-6]

One of the molecular nuclei common to our earlier studies is 7-amino-3-cephem (I). This bicyclic system is the fundamental moiety of the Δ^3-cephalosporins, compounds of major therapeutic importance.[7] The medicinal cephalosporins have a substituent, such as CH_3, at the 3 position, a carboxyl group at the 4 position, and an acylated 7-amino side chain. The β-lactam ring of the 3-cephem moiety is tipped up (toward the β face of the molecule) with respect to the dihydrothiazine ring.[7] The sulfur atom is also puckered about 0.9 Å above the rest of the atoms in the dihydrothiazine ring. Atomic coordinates for structure I are described elsewhere.[1]

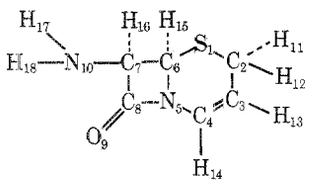

I

The purpose of this study is twofold. One is to view for the first time the spatial distribution of electrons in 7-amino-3-cephem using electron density maps. These are contour diagrams showing the topography of the electron clouds in selected planes through the molecule. We will examine the interesting regions of the sulfide lone pairs and S–C bonds, the ethylenic C=C bond, the enamine C–N bond, and the β-lactam C–N and C=O bonds. Plots of the total density of the valence electrons give a rather bulbous appearance to the electron clouds (see, *e.g.*, ref 8 and 9) and are not especially revealing about the details of bonding in the molecule. Of more interest than the total density map is the *difference map*, which is obtained by subtracting from the total density the spherically symmetric, ground state, valence electron atomic densities centered at the same positions as the atoms in the molecule.[9-12] The difference maps from valence electron wave functions display vividly and with frequent apparent qualitative validity the effects of bonding: lone-pair formation, σ and π bonding, and other descriptive concepts useful in chemistry.

The second purpose of this paper is to compare *via* electron density maps the EH[13-15] and CNDO/2D[11] methods. The EH wave function of 7-amino-3-cephem is obtained with previously published parameter values.[1] The CNDO/2D wave function is obtained by the standard CNDO/2 procedure[9,16] followed by a Löwdin $\mathbf{S}^{-1/2}$ transformation on the LCAO–MO coefficient matrix in order to renormalize the CNDO/2 wave function to the usual basis set of Slater-type orbitals.[9,11,17] We have incorporated the complete CNDO/2D algorithm into a single computer program called BNDO (big NDO) devised from CNINDO.[16] Comparisons of the way in which the EH and CNDO/2D methods distribute electrons in space have been published for adenine[11] and more recently for H_2S_2.[9,12,18] The EH and CNDO/2D shapes of the filled MO's of H_2S_2 were very similar in appearance, but the difference maps revealed contrasts between the bonding descriptions of these two methods. In addition, we have obtained difference maps from the EH and CNDO/2D methods for adamantane, bicyclo[2.2.2]octane, and *trans*-decalin. The hydrocarbon maps show gains in density along the C–C and C–H bond axes corresponding to σ bonding and losses of density from tetrahedral shaped regions around each carbon and spheroidal shaped regions around each hydrogen. Thus, the semiempirical findings on the large polycyclic alkanes are qualitatively similar to *ab initio* electron density maps of ethane.[19]

TABLE I: Net Atomic Charges in 7-Amino-3-cephem

Atom	EH	CNDO/2D	CNDO/2
S_1	−0.1313	0.0271	−0.1033
C_2	−0.0060	−0.1038	0.0080
C_3	−0.2222	−0.0629	−0.0638
C_4	0.1268	0.1109	0.1049
N_5	−0.1563	−0.2633	−0.1365
C_6	0.2363	0.0012	0.0741
C_7	0.1671	0.0446	0.0594
C_8	0.8214	0.4248	0.3390
O_9	−0.9477	−0.3501	−0.3065
N_{10}	−0.6270	−0.3100	−0.1952
H_{11}	0.0527	0.0423	0.0165
H_{12}	0.0511	0.0463	0.0196
H_{13}	0.0615	0.0352	0.0105
H_{14}	0.0448	0.0262	−0.0005
H_{15}	0.0289	0.0417	0.0108
H_{16}	0.0446	0.0184	−0.0072
H_{17}	0.2273	0.1327	0.0825
H_{18}	0.2281	0.1385	0.0875

[a] The fourth decimal place in these data, as well as those in Table II, is without much significance because of minor round-off errors which can enter from the input atomic coordinates, convergence criterion, conversion factors, etc., even though the calculations are carried out in double precision.

TABLE II: Mulliken Overlap Populations in 7-Amino-3-cephem

Bond	EH	CNDO/2D	Bond	EH	CNDO/2D
S_1–C_2	0.6690	0.5326	C_7–N_{10}	0.7012	0.6866
S_1–C_6	0.7158	0.4750	C_2–H_{11}	0.7966	0.7299
C_2–C_3	0.8104	0.8747	C_2–H_{12}	0.7985	0.7334
C_3=C_4	1.2483	1.2675	C_3–H_{13}	0.8004	0.7605
C_4–N_5	0.8520	0.7502	C_4–H_{14}	0.8072	0.7716
N_5–C_6	0.6939	0.6714	C_6–H_{15}	0.8183	0.7440
C_6–C_7	0.6771	0.7484	C_7–H_{16}	0.7971	0.7146
C_7–C_8	0.8017	0.7926	N_{10}–H_{17}	0.7485	0.6101
C_8=O_9	0.9856	0.7918	N_{10}–H_{18}	0.7480	0.6167
N_5–C_8	0.9151	0.7057			

Results and Discussion

The gross charge distribution of 7-amino-3-cephem can be seen in the conventional Mulliken[20] population analysis results (Tables I and II). Most of the charges from the three MO methods are reasonable relative to each other, but there are two nonhydrogenic atoms (S_1 and C_2) whose CNDO/2 net atomic charges change sign due to deorthogonalization. Such sign reversals are not too common for nonhydrogenic atoms.[11,21] Previous experience[9,11] indicated that deorthogonalization renders the apparent net atomic charges from a CNDO/2 wave function closer to EH values, but such is not the case for many of the atoms of 7-

amino-3-cephem. The sign reversals in the net charges of S_1 and C_2 are due to the electron density in the S 3p and 3d AO's being partitioned onto the secondary carbon C_2 by the prescription of the deorthogonalization. Differences in directionality of EH and CNDO/2D lone pair regions, which are discussed below, are not apparent from the orbital populations, thus exemplifying the superior acuity of electron density maps compared to a population analysis. The CNDO/2D charges on the hydrogens are expectedly more positive than the CNDO/2 values.[9] The EH and CNDO/2D overlap populations are quite similar for most bonds in the molecule (Table II), but the two wave functions differ in their predictions about the relative strengths of the S_1–C_2 and S_1–C_6 bonds. The lengths of these bonds from X-ray crystallographic data[7] are very close (1.82 and 1.79 Å, respectively), indicating that the EH results better reproduce this subtle difference. The CNDO/2D population analysis is thus yielding misleading results regarding the S–C bonds, perhaps due to the treatment of the S 3d atomic orbitals (*vide infra*).

Electron density maps of 7-amino-3-cephem in Figures 1–7 have contour labels corresponding to the following densities: T or 8 for 0.09, S or 7 for 0.009, and R or 6 for 0.0009 e/bohr ^{3}. The lettered contours correspond to regions where there is greater density in the molecule than in the sum of the constituent atomic densities and may be associated with bonding or lone-pair regions. Numbered contours specify regions where the molecular density is *lower* than in the atoms. The dotted contours (.,) delineate where the molecular and atomic densities are equal. Some contours may appear discontinuous, but this is only an artifact of the limited resolution of the characters of the computer printout. The effects of formation of a molecule from the constituent atoms are most prominent within about 1.8 Å of the nuclei. Consequently, Figures 1–6 cover 3.6 × 4.8 Å, and Figures 7 covers 4.8 × 6.4 Å. Positions or projections of positions of the nuclei on the plane of density calculation are denoted by asterisks. Solid lines connect bonded atoms lying in the plane of calculation of each map; projections of internuclear axes between other bonded atoms within the field of each map are shown by dashed lines. Calculation of Figures 1–7 from the MO's required 44 min on the IBM 370/158 computer.

The buildups seen in Figure 1 on the α (bottom) and β (top) faces of the sulfur mark the regions occupied by the two sulfur lone pairs. A surprising difference between the EH and CNDO/2D maps is to be noted. Whereas CNDO/2D generally produces a smoother charge distribution than EH due to the explicit inclusion of interelectronic repulsions, CNDO/2D gives greater directionality to the lone-pair lobes. CNDO/2D gives a cloven lone-pair region concentrated along the two axes associated with sp^3 hybridization at sulfur. The EH map is suggestive of sp^2,p hybridization like the combined shapes of the individual lone-pair MO's of a simple sulfide. A similar contrast between EH and CNDO/2D was seen in the study of H_2S_2.[9,12,18] Density maps from an *ab initio* wave function of H_2S[22] showed more directionality of the lone-pair lobes than seen in the EH map of Figure 1, but also showed more density buildup in the plane of the R–S–R group than seen in the CNDO/2D map of Figure 1. A final point to notice about Figure 1 is that there is only density loss throughout the middle of

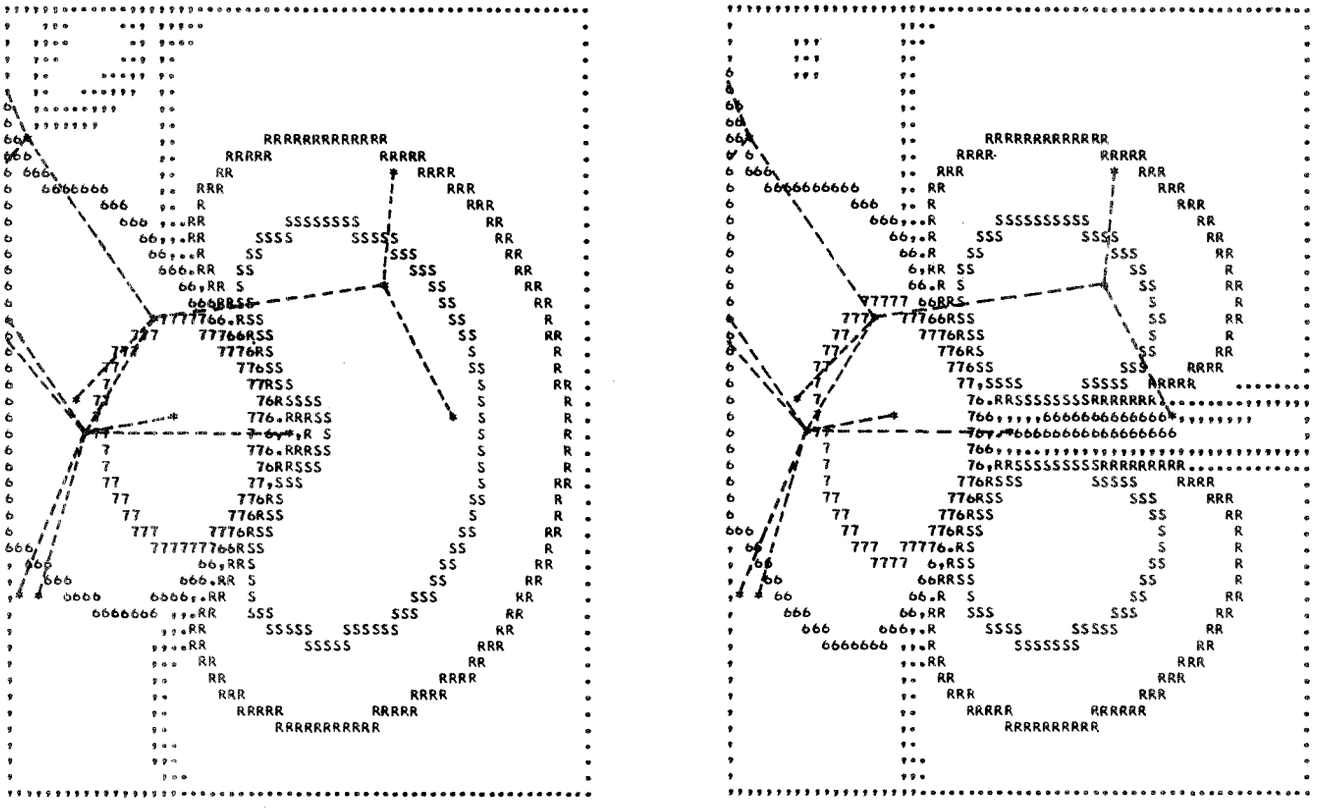

Figure 1. EH (left) and CNDO/2D (right) difference maps of 7-amino-3-cephem computed in the plane through the sulfur and perpendicular to the $C_2 \cdots C_6$ axis. This view looks down the $C_2 \cdots C_6$ axis, so that C_2 and C_6 fall at the same point, and S_1 is to the right of this point near the center of the maps. The β face of the molecule is toward the top of the maps. The peaks in density gain in the lone-pair lobes are 0.0715 and 0.0675 e/bohr^3 in the EH and CNDO/2D maps, respectively.

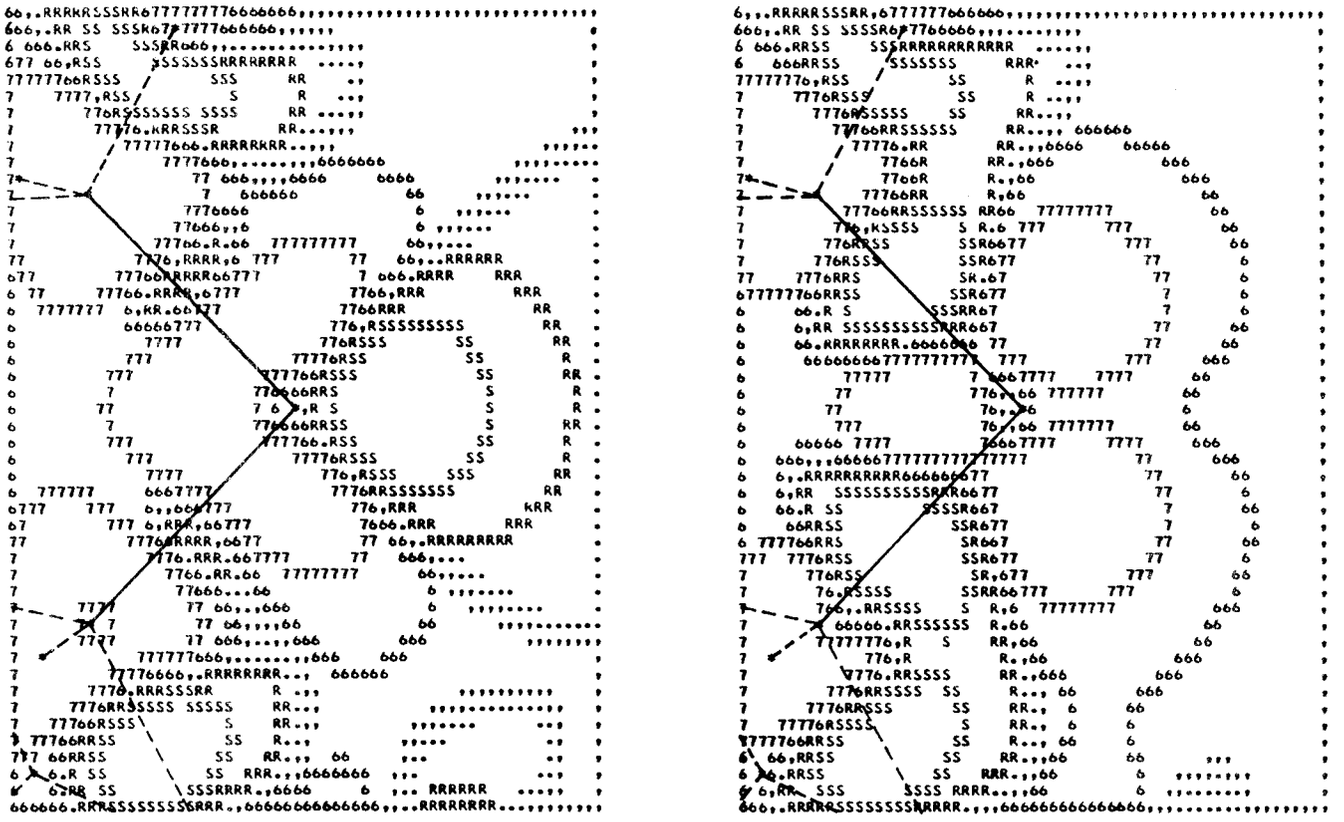

Figure 2. EH (left) and CNDO/2D (right) difference maps of 7-amino-3-cephem computed in the plane of C_6–S_1–C_2. The projection of the β-lactam ring falls in the lower left-hand corner.

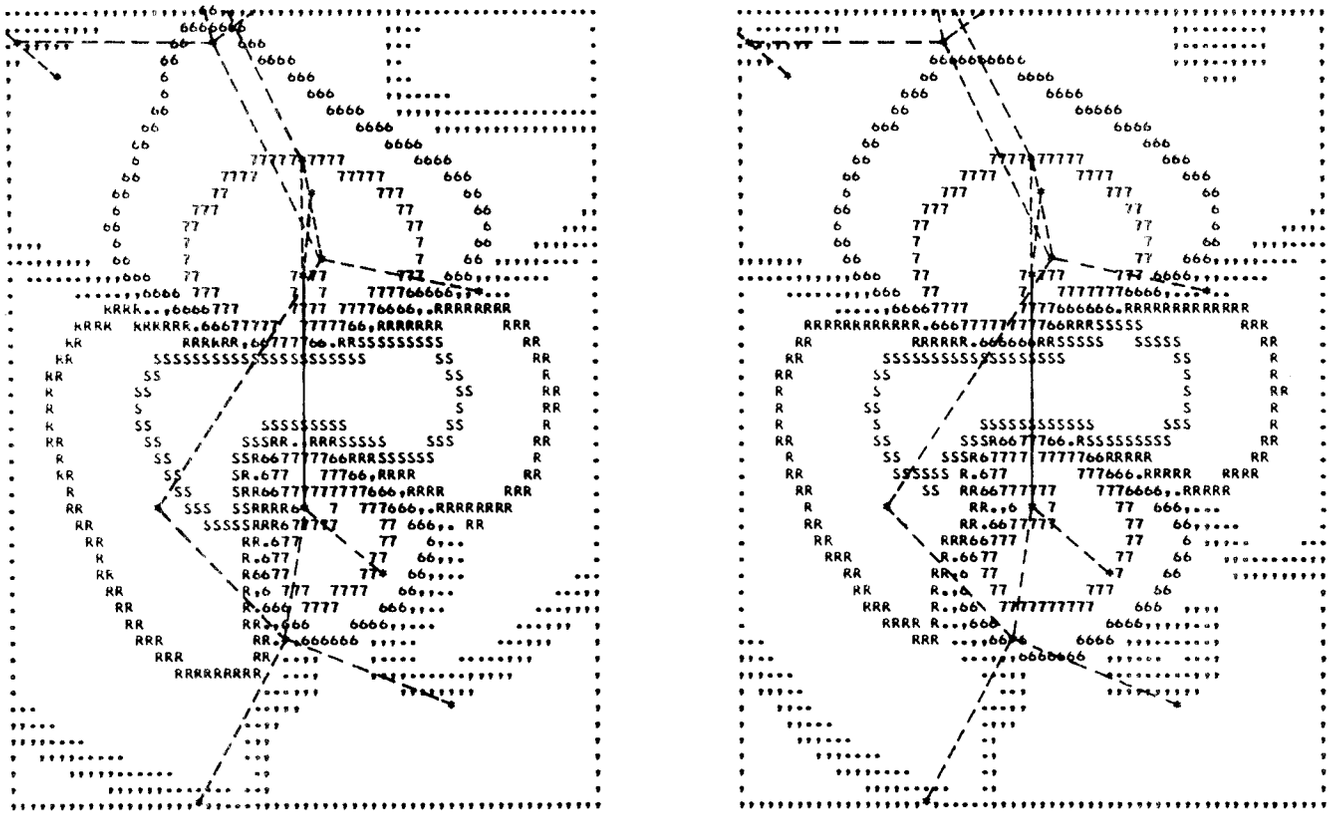

Figure 3. EH (left) and CNDO/2D (right) difference maps of 7-amino-3-cephem computed in the plane which passes through the C_3–C_4 axis and is perpendicular to the C_3–C_4–N_5 plane. The C_3–C_4 axis is the vertical solid line at the center of the maps. The projection of the β-lactam ring extends off the top of the maps. The β face of the molecule is toward the left.

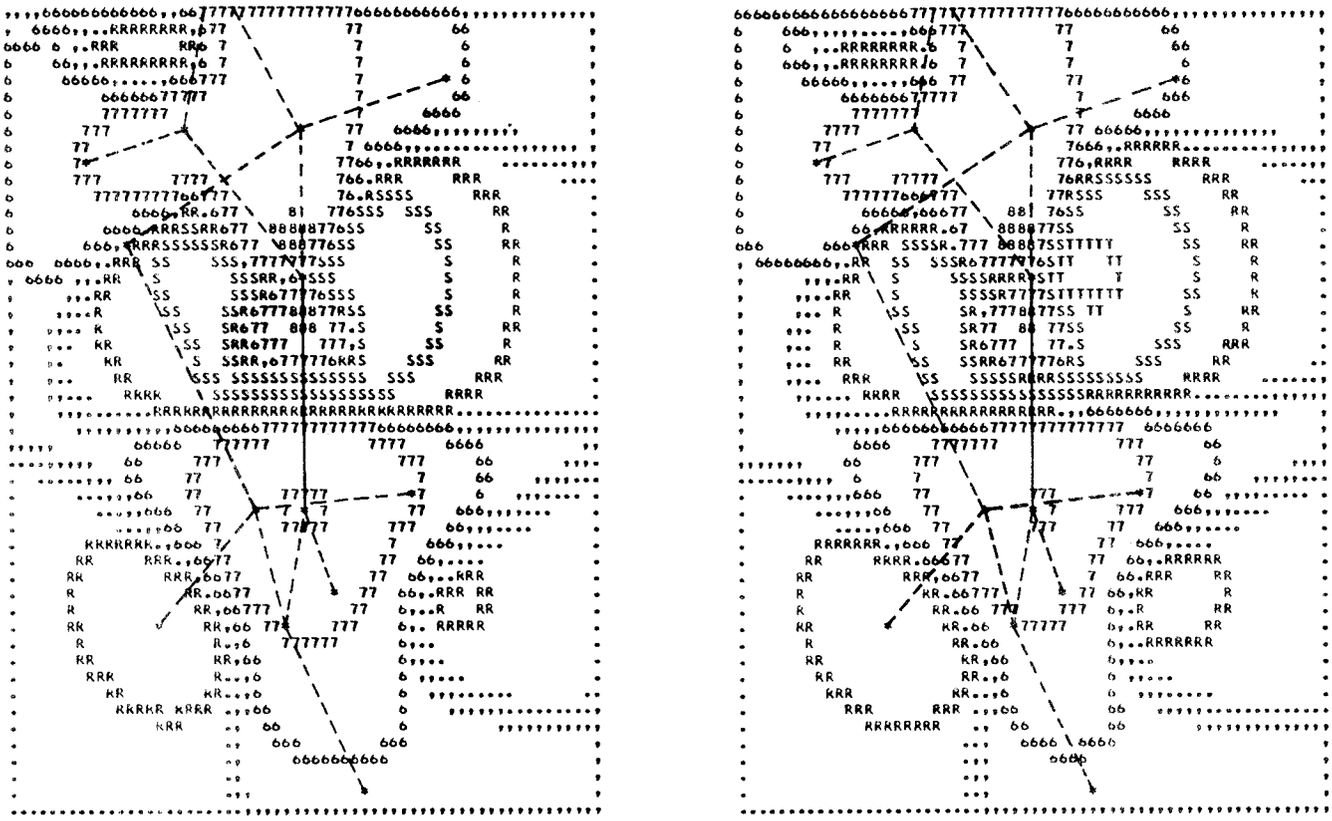

Figure 4. EH (left) and CNDO/2D (right) difference maps of 7-amino-3-cephem computed in the plane which passes through the C_4–N_5 axis (solid line) and is perpendicular to the C_4–N_5–C_6 plane. The β face of the molecule is toward the left, and the projection of the β-lactam ring extends off the top of the maps.

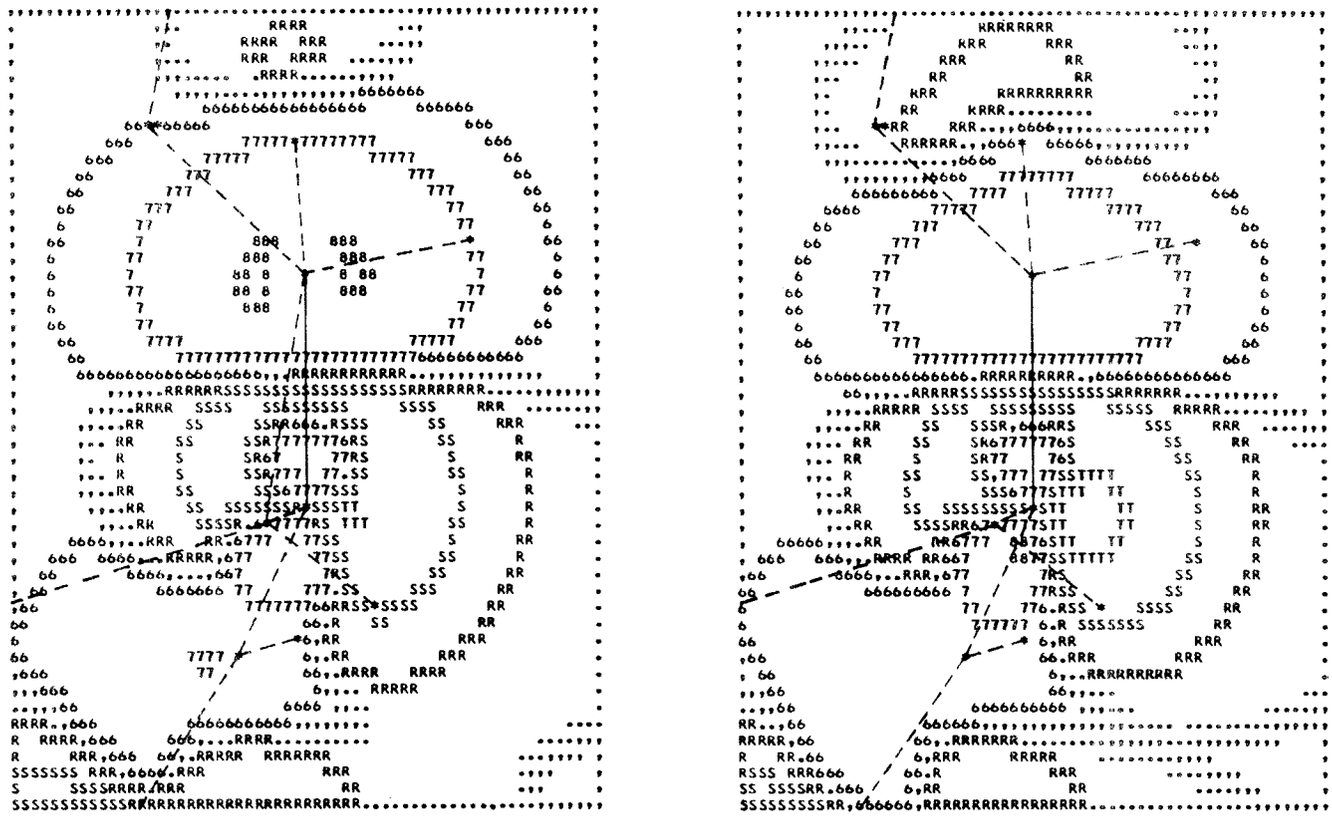

Figure 5. EH (left) and CNDO/2D (right) difference maps of 7-amino-3-cephem computed in the plane which passes through the N_5–C_8 axis (solid line) and is perpendicular to the N_5–C_8–C_7 plane. The projection of the dihydrothiazine ring extends off the lower left-hand corner of the maps. The β face of the molecule is toward the left. In this view C_8 and C_7 fall at the same asterisk. The peaks in density in the N_5 lone-pair lobe are 0.1029 and 0.2022 e/bohr^3 in the EH and CNDO/2D maps, respectively.

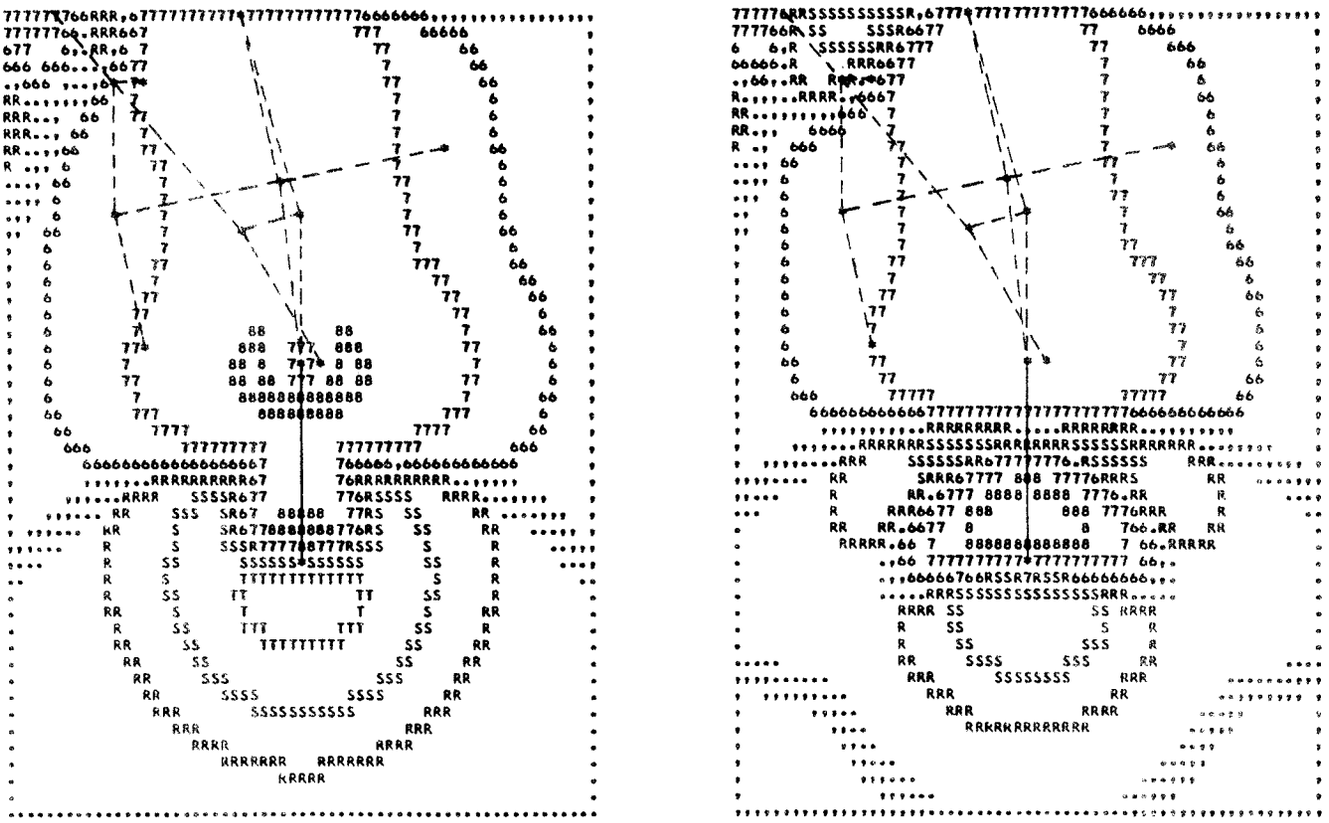

Figure 6. EH (left) and CNDO/2D (right) difference maps of 7-amino-3-cephem computed in the plane which passes through the O_9–C_8 axis (solid line) and is perpendicular to the O_9–C_8–N_5 plane. The projection of the dihydrothiazine ring extends off the top of the maps, and the β face of the molecule is toward the left. H_{17} of the amino group and C_3 happen to fall at the same asterisk in the upper left-hand corner of the maps.

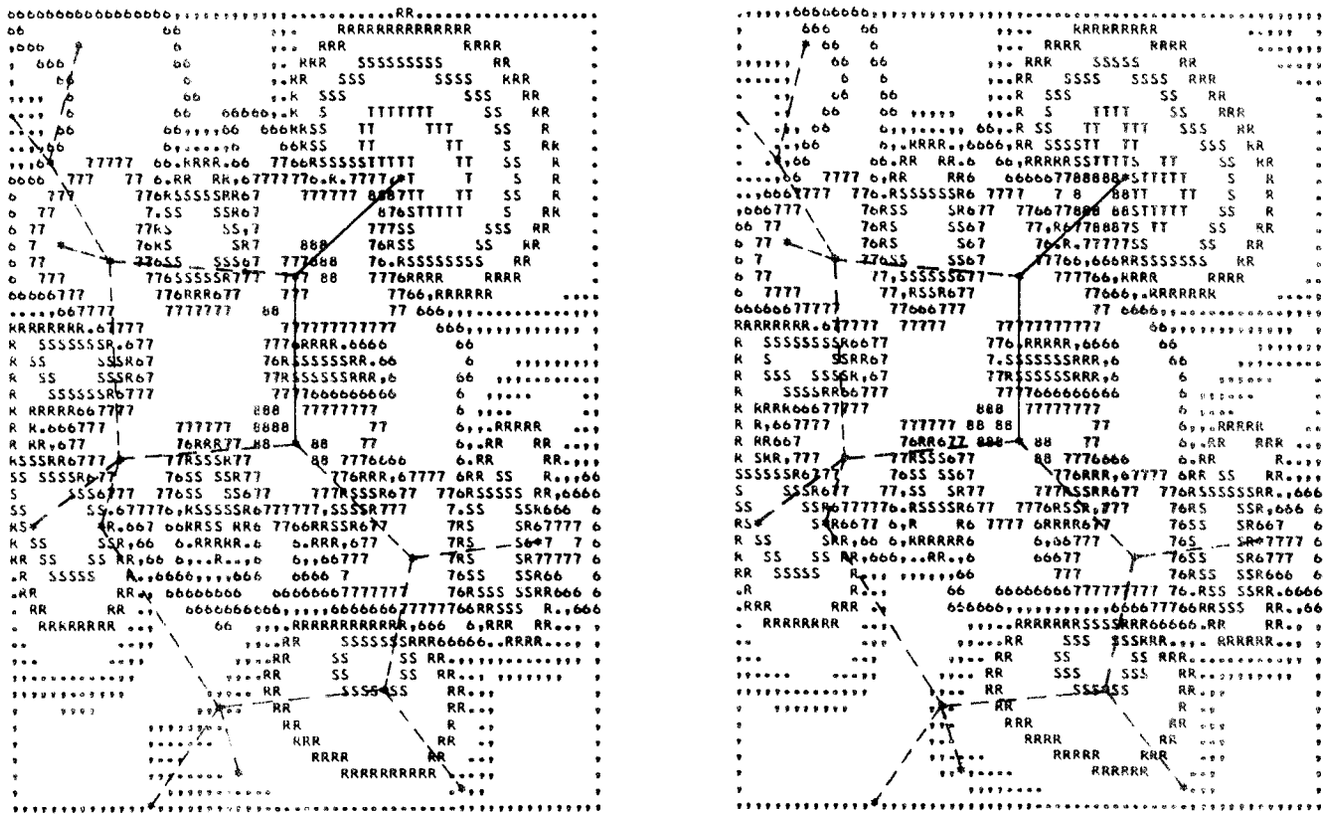

Figure 7. EH (left) and CNDO/2D (right) difference maps of 7-amino-3-cephem in the plane of N_5–C_8–O_9. This plane also slices through the regions near several other nuclei including C_4 (0.34 Å out of the plane), H_{14} (0.13 Å), C_6 (0.36 Å), C_7 (0.12 Å), and H_{15} (0.27 Å). The peaks in density in the O_9 lone-pair lobe are 0.3068 and 0.3026 e/bohr^3 in the EH and CNDO/2D maps, respectively.

the dihydrothiazine ring, meaning that transannular bonding is not great in the ground state of the molecule. The excited states also have little transannular character.[1]

The gains along the S–C axes in Figure 2 correspond to σ bonding. The lack of any accumulation of sulfur lone-pair electrons in the plane of C_6–S_1–C_2 is evident in the CNDO/2D map. CNDO/2D puts much more density in the S–C σ bonding regions than does the EH method. Thus, the density maps indicate that CNDO/2D gives stronger S–C bonds compared to EH, which is contrary to the conclusion that would have been surmised from the overlap populations of Table II. The two S–C bonds appear very similar. The volume of density loss around C_2 and C_6 is roughly tetrahedrally shaped.

Figure 3 reveals that electrons have aggregated along the C_3–C_4 axis (σ bonding), as well as on either side of the C_3=C_4–N_5 plane (π bonding). The π cloud is more extensive on the β face of the molecule. The density buildup between the doubly bonded carbons is not unlike that which X-ray crystallographers have tried to see in their electron density maps.[23] The density difference maps do not show a banana-type π bond between C_3 and C_4, but perhaps if the σ density were separable from the π (which it is not due to the slight nonplanarity of the ethylenic moiety) then such bonding would become apparent. Compared to the separated atoms, electrons are lost from the immediate vicinity of each carbon. The loss from around C_4 is seen to be greater than from around C_3, which fits with the positive net atomic charge of the former and negative net atomic charge of the latter (Table I). The EH and CNDO/2D charge distributions in the region of the molecule covered by Figure 3 are remarkably similar.

The C_4–N_5 bond (Figure 4) is the one spanned by an enamine π MO important to the uv absorption of cephalosporins.[1] The EH and CNDO/2D maps yield similar results: there is a small accumulation of electron density on the C–N axis (σ bonding) and considerable gain on either side of this axis (π bonding), which is contiguous with the β-lactam nitrogen lone pair. The N_5 lone pair extends mainly toward the α face of the molecule, but the density buildup on the other face is by no means negligible. No doubt this distribution at N_5 accounts for the partial conjugation of the β-lactam and dihydrothiazine rings and for the effects of substituents at certain positions in the dihydrothiazine ring affecting the chemistry of the β-lactam ring. As in the case of the sulfur lone pairs, the CNDO/2D method concentrates more density along the lone-pair axis on the β face than does the EH method.

Figures 5 and 6 show the density in two planes passing perpendicularly through the N_5–C_8=O_9 plane of the β-lactam ring, and Figure 7 shows the density in the latter plane. The lone-pair density buildup around N_5 is again noted to be hatchet-head shaped with the larger accumulation on the α face of the molecule (Figure 5). CNDO/2D gives a density peak twice as high as the EH method near N_5. The lone-pair region on the carbonyl oxygen O_9 appears as a nub over the end of the C=O bond. The EH and CNDO/2D descriptions of the O_9 lone-pair regions are distinctly different in shape. In the plane perpendicular to the β-lactam amide group (Figure 6) the CNDO/2D wave function puts much less density at the end of the carbonyl group. In the plane of the β-lactam amide group (Figure 7), CNDO/2D has the O_9 lone-pair region somewhat polarized into two fused lobes. This suggests that the two oxygen lone pairs are principally in sp^2-like hybrid orbitals lying in the O_9=C_8–N_5 plane. EH fails to show more than a kidney-shaped nub of density gain on the carbonyl oxygen, and also fails to show any C–O σ bonding. In fact, the CNDO/2D wave function has much more π, as well as σ, bonding density in the carbonyl bond. In this regard, electron density difference maps of carbon monoxide obtained from *ab initio* wave functions[17,24–26] resemble more closely the CNDO/2D description of the β-lactam carbonyl bond than the EH one. As is evident in Figures 5–7, the charge separation between C_8 and O_9 is much less in the CNDO/2D description, and this fact is apparent in the net atomic charges (Table I). The overlap populations of the C_8=O_9 bond (Table II) do not properly reflect the relative amounts of density in this bond as predicted by the two MO methods.

Electron density plots from both semiempirical methods reveal in Figure 7 various σ bonds of the β-lactam ring, the N_5–C_4 σ bond, and the C_4–H_{14} σ bond, all of which lie in or close to the plane being mapped. Of special interest is that the σ-bonding electron density peaks for the ring bonds lie mostly outside the four-membered ring. In other strained systems a similar phenomenon is observed. For instance, in a cyclopropylidene ring, we have seen the so-called bent C–C bonds.[27] There are many instances where the bent bonds of cyclopropane have been viewed with electron density maps.[28,29] Bent bonds are evident in the four-membered rings of cubane.[30]

In regard to biological activity, the most interesting part of our model compound is the β-lactam ring. This is the portion of cephalosporin molecules which can acylate some bacterial cell wall enzyme and destroy the bacteria, or, conversely, be hydrolyzed by a bacterial β-lactamase and itself be destroyed.[7] Apparent in Figures 5 and 6 is the great loss of electron density around the carbonyl carbon C_8. This loss corresponds to the large positive net atomic charge on this atom (Table I) and relates to the susceptibility of this center to nucleophilic attack. An approaching nucleophile, such as RS^-, OH^-, or H_2O, could easily approach C_8 from either the α or β faces. Electronically, the two modes of attack are not much different, but sterically, other parts of the molecule can partially block one or both paths.[6,31,32] The lone-pair buildups on O_9 and N_5 are seen in Figures 5 and 6 to be spatially disposed such that they would not intercept a nucleophile approaching C_8. Also, there is loss through most of the transannular region of the β-lactam ring (Figures 6 and 7). These factors help explain the reactivity of the β-lactam ring.

Conclusion

From illustrations in the present study, characteristics of the EH and CNDO/2D MO methods and of the Mulliken population analysis on the diverse group of chemical functionalities in 7-amino-3-cephem have been scrutinized. Electron density maps are more useful than the population analysis in assessing details of electron topography, such as lone pair directionality and relative bond populations. Also, we have seen how the electrons distribute themselves about these functionalities, so that the chemical, physical, and biological properties of cephalosporins can be better appreciated. In subsequent papers, the electronic structures of some of the clinically useful cephalosporins and other β-lactam compounds will be explored.

Acknowledgments. Discussions with M. M. Marsh and the assistance of D. E. Presti with the computer calculations are gratefully acknowledged.

References and Notes

(1) D. B. Boyd, *J. Amer. Chem. Soc.*, **94**, 6513 (1972).
(2) D. B. Boyd, *J. Med. Chem.*, **16**, 1195 (1973).
(3) J. L. Strominger, *Johns Hopkins Med. J.*, **133**, 63 (1973).
(4) R. B. Hermann, *J. Antibiot.*, **26**, 223 (1973).
(5) W. C. Topp and B. G. Christensen, *J. Med. Chem.*, **17**, 342 (1974).
(6) D. B. Boyd, R. B. Hermann, D. E. Presti, and M. M. Marsh, to be submitted for publication; paper IV.
(7) E. H. Flynn, "Cephalosporins and Penicillins: Chemistry and Biology," Academic Press, New York, N.Y., 1972.
(8) O. Martensson, *Acta Chem. Scand.*, **25**, 3763 (1971).
(9) D. B. Boyd, *J. Phys. Chem.*, **78**, 1554 (1974). This paper was part XI of the series "Mapping Electron Density in Molecules," of which the present paper is part XII.
(10) D. B. Boyd, *Theor. Chim. Acta*, **18**, 184 (1970).
(11) D. B. Boyd, *J. Amer. Chem. Soc.*, **94**, 64 (1972), and references therein.
(12) D. B. Boyd, *Theor. Chim. Acta*, **30**, 137 (1973).
(13) R. Hoffmann and W. N. Lipscomb, *J. Chem. Phys.*, **36**, 2179, 3489 (1962); **37**, 2872 (1962).
(14) R. Hoffmann, *J. Chem. Phys.*, **39**, 1397 (1963); **40**, 2480 (1964).
(15) D. B. Boyd and W. N. Lipscomb, *J. Theor. Biol.*, **25**, 403 (1969).
(16) J. A. Pople and D. L. Beveridge, "Approximate Molecular Orbital Theory," McGraw-Hill, New York, N.Y., 1970.
(17) F. A. Van-Catledge, *J. Phys. Chem.*, **78**, 763 (1974).
(18) D. B. Boyd, *Int. J. Quantum Chem., Quantum Biology Symp.*, **No. 1**, 13 (1974); *J. Amer. Chem. Soc.*, **94**, 8799 (1972). Regarding the correlation of predicted S–S bond strength and Raman stretching frequency in the first citation, see recent corroborative evidence in paper by H. E. Van Wart, L. L. Shipman, and H. A. Scheraga, *J. Phys. Chem.*, **78**, 1848 (1974).
(19) R. M. Pitzer and W. N. Lipscomb, *J. Chem. Phys.*, **39**, 1995 (1963).
(20) R. S. Mulliken, *J. Chem. Phys.*, **23**, 1833 (1955).
(21) D. D. Shillady, F. P. Billingsley, II, and J. E. Bloor, *Theor. Chim. Acta*, **21**, 1 (1971).
(22) D. B. Boyd, *J. Chem. Phys.*, **52**, 4846 (1970).
(23) R. B. Helmholdt, A. F. J. Ruysink, H. Reynaers, and G. Kemper, *Acta Crystallogr., Sect. B*, **28**, 318 (1972).
(24) R. F. W. Bader and A. D. Bandrauk, *J. Chem. Phys.*, **49**, 1653 (1968).
(25) M. J. Hazelrigg, Jr., and P. Politzer, *J. Phys. Chem.*, **73**, 1008 (1969).
(26) D. A. Kohl and L. S. Bartell, *J. Chem. Phys.*, **51**, 2896 (1969).
(27) D. B. Boyd and R. Hoffmann, *J. Amer. Chem. Soc.*, **93**, 1064 (1971).
(28) O. Martensson and G. Sperber, *Acta Chem. Scand.*, **24**, 1749 (1970).
(29) R. M. Stevens, E. Switkes, E. A. Laws, and W. N. Lipscomb, *J. Amer. Chem. Soc.*, **93**, 2603 (1971).
(30) O. Martensson, *Acta Chem. Scand.*, **24**, 1495 (1970).
(31) P. P. K. Ho, R. D. Towner, J. M. Indelicato, W. A. Spitzer, and G. A. Koppel, *J. Antibiot.*, **25**, 627 (1972).
(32) P. P. K. Ho, R. D. Towner, J. M. Indelicato, W. J. Wilham, W. A. Spitzer, and G. A. Koppel, *J. Antibiot.*, **26**, 313 (1973).

Ultrasound Propagation in Binary Mixtures of Dimethyl Sulfoxide and Water

D. E. Bowen,* M. A. Priesand, and M. P. Eastman

The University of Texas at El Paso, El Paso, Texas 79968

(Received June 24, 1974)

Publication costs assisted by The University of Texas at El Paso

Measurements of the velocity and attenuation of sound have been made for the dimethyl sulfoxide (DMSO)–water binary system as a function of composition and temperature. It has been found that the velocity and attenuation *vs.* composition curves peak in the region $X_{DMSO} \sim 0.3$ for all temperatures studied. No characteristic relaxation frequency was observed for this binary system in the frequency range studied (6–26 MHz). Values for the adiabatic compressibility have been calculated from the velocity measurements and previously published densities. The compressibility decreases rapidly in the region of low DMSO concentration and peaks at $X_{DMSO} \sim 0.3$. The experimental results are discussed in terms of the formation of thermolabile nonstoichiometric 1:2 complexes and recent theories of the structure of water.

I. Introduction

In recent years the dimethyl sulfoxide–water system has been investigated by a wide variety of experimental techniques. These studies have been undertaken because the DMSO–H_2O system is useful as a solvent and as a reaction medium and because DMSO exhibits a number of interesting properties when interacting with biological systems.[1-6] The results of neutron inelastic scattering (nis) experiments have indicated that DMSO is an associated dipolar liquid and that the methyl groups in the DMSO molecule do not take part in hydrogen bonding as had been suggested.[7] In solutions of DMSO–H_2O containing small amounts of DMSO nis and X-ray diffraction data provide evidence for an increased ordering of water molecules. Apparently, however, this increase in molecular order is not accompanied by a change in hydrogen bond energies or by a large change in the distribution of hydrogen bond energies.[7-9] Thus, it seems that there is no clathrate or "iceberg" formation in aqueous solutions containing small amounts of DMSO and that the effect of DMSO on the water structure is not such as to produce a decrease in the so-called "structural temperature" of the water.[8]

In solutions containing larger concentrations of DMSO there is evidence for the breaking down of the water structure and for the formation of hydrogen bonded thermolabile DMSO–H_2O complexes.[7-10] Studies of the DMSO–H_2O system by a variety of experimental techniques indicate that the effect of this complex formation is greatest in the region where the H_2O–DMSO molar ratio is about 2:1.[11-14] However, at present there is no evidence for the formation of a DMSO–H_2O complex having a definite stoichiometry.[10] Nmr measurements show that complex formation leads to reduced translational and rotational mobility for both DMSO and water with the mobility minimum occurring at $X_{DMSO} = 0.35$.[14]

The purpose of this paper is to investigate the DMSO–H_2O system by means of ultrasonic velocity and attenuation measurements.[15] Particular emphasis is placed on